doi:10.1093/brain/awt344 Brain 2014: 137; 537–552 | 537

BRAIN
A JOURNAL OF NEUROLOGY

Inositol trisphosphate 3-kinase B is increased in human Alzheimer brain and exacerbates mouse Alzheimer pathology

Virginie Stygelbout,[1,2,3] Karelle Leroy,[3] Valérie Pouillon,[1,2] Kunie Ando,[4] Eva D'Amico,[1,2] Yonghui Jia,[5,6] H. Robert Luo,[5,6] Charles Duyckaerts,[4] Christophe Erneux,[1] Stéphane Schurmans[1,2,7,8,9,*] and Jean-Pierre Brion[3,*]

1 Institut de Recherches Interdisciplinaires en Biologie Humaine et Moléculaire, Université Libre de Bruxelles, 6041-Gosselies, Belgium
2 Institut de Biologie et de Médecine Moléculaires, Université Libre de Bruxelles, 6041-Gosselies, Belgium
3 Laboratoire d'Histologie, de Neuroanatomie et de Neuropathologie, Université Libre de Bruxelles, 1070-Bruxelles, Belgium
4 Laboratoire de Neuropathologie Escourolle and Centre de Recherche de l'ICM, Hôpital de la Pitié-Salpêtrière, AP-HP, 75013-Paris, France
5 Department of Pathology, Harvard Medical School, Dana-Farber/Harvard Cancer Centre, MA02115, Boston, USA
6 Department of Laboratory Medicine, Children's Hospital Boston, MA02115, Boston, USA
7 Laboratoire de Génétique Fonctionnelle, GIGA-Research Centre, Université de Liège, 4000-Liège, Belgium
8 Secteur de Biochimie Métabolique, Département des Sciences Fonctionnelles, Université de Liège, 4000-Liège, Belgium
9 Welbio, Université de Liège, 4000-Liège, Belgium

*These authors contributed equally to this work.

Correspondence to: S. Schurmans,
Laboratoire de Génétique Fonctionnelle,
GIGA-Research Centre,
Building 34,
Université de Liège,
rue de l'Hôpital 1,
4000-Liège,
Belgium
E-mail: sschurmans@ulg.ac.be

ITPKB phosphorylates inositol 1,4,5-trisphosphate into inositol 1,3,4,5-tetrakisphosphate and controls signal transduction in various hematopoietic cells. Surprisingly, it has been reported that the *ITPKB* messenger RNA level is significantly increased in the cerebral cortex of patients with Alzheimer's disease, compared with control subjects. As extracellular signal-regulated kinases 1/2 activation is increased in the Alzheimer brain and as ITPKB is a regulator of extracellular signal-regulated kinases 1/2 activation in some hematopoietic cells, we tested whether this increased activation in Alzheimer's disease might be related to an increased activity of ITPKB. We show here that ITPKB protein level was increased 3-fold in the cerebral cortex of most patients with Alzheimer's disease compared with control subjects, and accumulated in dystrophic neurites associated to amyloid plaques. In mouse Neuro-2a neuroblastoma cells, *Itpkb* overexpression was associated with increased cell apoptosis and increased β-secretase 1 activity leading to overproduction of amyloid-β peptides. In this cellular model, an inhibitor of mitogen-activated kinase kinases 1/2 completely prevented overproduction of amyloid-β peptides. Transgenic overexpression of ITPKB in mouse forebrain neurons was not sufficient to induce amyloid plaque formation or tau hyperphosphorylation. However, in the 5X familial Alzheimer's disease mouse model, neuronal ITPKB overexpression significantly increased extracellular signal-regulated kinases 1/2 activation and β-secretase 1 activity, resulting in exacerbated Alzheimer's disease pathology as shown by increased astrogliosis, amyloid-β_{40} peptide production and tau hyperphosphorylation. No impact on pathology was

Received January 7, 2013. Revised October 16, 2013. Accepted October 25, 2013. Advance Access publication January 8, 2014
© The Author (2014). Published by Oxford University Press on behalf of the Guarantors of Brain. All rights reserved.
For Permissions, please email: journals.permissions@oup.com

Downloaded from https://academic.oup.com/brain/article/137/2/537/283818 by guest on 23 April 2024

observed in the 5X familial Alzheimer's disease mouse model when a catalytically inactive ITPKB protein was overexpressed. Together, our results point to the ITPKB/inositol 1,3,4,5-tetrakisphosphate/extracellular signal-regulated kinases 1/2 signalling pathway as an important regulator of neuronal cell apoptosis, APP processing and tau phosphorylation in Alzheimer's disease, and suggest that ITPKB could represent a new target for reducing pathology in human patients with Alzheimer's disease with ITPKB expression.

Keywords: Alzheimer pathology; inositol phosphates; ITPKB; inositol (1,3,4,5) tetrakisphosphate

Abbreviations: CTF = carboxy terminal fragment; ERK = extracellular signal-regulated kinases; 5XFAD mouse = heterozygote mouse expressing five familial Alzheimer's disease mutations for APP and PSEN1; HA = haemagglutinin; Ins(1,3,4,5)P4 = inositol 1,3,4,5-tetrakisphosphate; Ins(1,4,5)P3 = inositol 1,4,5-trisphosphate; MEK = mitogen-activated protein kinase kinase; 2Tg = 2Tg Camk2a-tTA/HA-Itpkb

Introduction

Alzheimer's disease is a neurodegenerative disease characterized by a loss of neurons in the cerebral cortex and the hippocampus associated with the presence of extracellular amyloid plaques and intracellular neurofibrillary tangles. Although 1–2% of Alzheimer's disease cases are a result of pathogenic mutations in amyloid precursor protein (APP) and presenilin 1/2 (*PSEN1/2*) genes, most of the cases are sporadic and likely result from pathogenic interactions between multiple factors including APP/amyloid-β, tau, apolipoprotein E genotype, ageing and genetic variants (Huang *et al*., 2012). Recently, genome-wide association studies have identified allelic variants of several genes that constitute risk factors for sporadic Alzheimer's disease (Harold *et al*., 2009; Lambert *et al*., 2009). Emilsson *et al*. (2006) reported that messenger RNA levels of inositol (1,4,5) trisphosphate 3-kinase B (*ITPKB*) are 2.6- to 4.4-fold increased in the frontal cortex of 61 patients with Alzheimer's disease compared with 53 control individuals (Emilsson *et al*., 2006). Real-time reverse transcription-PCR on each individual separately confirmed these microarray experiments.

Inositol trisphosphate 3-kinases convert inositol 1,4,5-trisphosphate [Ins(1,4,5)P3] into inositol 1,3,4,5-tetrakisphosphate [Ins(1,3,4,5)P4] (Communi *et al*., 1995; Irvine *et al*., 2001). In mammalian cells, three isoforms of inositol trisphosphate 3-kinase exist, designated ITPKA, ITPKB and ITPKC. These three isoforms share a well-conserved carboxy-terminal catalytic domain, an inositol trisphosphate and an adenosine triphosphate binding motif, as well as a calmodulin binding domain (Communi *et al*., 1995; Vanweyenberg *et al*., 1995; Irvine *et al*., 2001; York *et al*., 2001; Pattni *et al*., 2004). The gene encoding ITPKB is expressed ubiquitously (Hascakova-Bartova *et al*., 2004). ITPKB is clearly involved in hematopoietic cell development and function. Indeed, ITPKB inactivation leads to altered thymocyte development and a nearly complete absence of peripheral T cells (Pouillon *et al*., 2003; Wen *et al*., 2004). B cell, natural killer cell and neutrophil development and function were also altered in ITPKB-deficient mice (Jia *et al*., 2007, 2008; Maréchal *et al*., 2007, 2011; Miller *et al*., 2007; Sauer *et al*., 2013). Mechanistically, in hematopoietic cells, Ins(1,3,4,5)P4—a water-soluble compound—probably acts as a signalling molecule by competing with membrane phosphoinositides for binding to pleckstrin homology domain-containing proteins such as RASA3 and protein kinase B. Thus, upon cell stimulation, cytosolic Ins(1,3,4,5)P4 prevents the subcellular relocalization of RASA3 and protein kinase B from the cytosol to the plasma membrane (Wen *et al*., 2004; Jia *et al*., 2007; Maréchal *et al*., 2007). Indeed, in lymphocytes, ITPKB inactivation is associated with a decreased extracellular signal-regulated kinases 1/2 (ERK1/2) activation, a probable consequence of an increased relocalization of RASA3, a RAS GTPase-activating protein at the plasma membrane, close to RAS, its substrate (Wen *et al*., 2004; Maréchal *et al*., 2007). An increased ERK1/2 activation has been reported in Alzheimer's disease, which might be related to an increased activity of ITPKB (Arendt *et al*., 1995; Perry *et al*., 1999; Ferrer *et al*., 2001).

To investigate this hypothesis, we first analysed ITPKB protein expression and localization in the cerebral cortex of patients with Alzheimer's disease and of control individuals. Second, we analysed the impact of increased ITPKB protein expression on Alzheimer's disease pathology in cultured cells and in transgenic mice.

Materials and methods

Human tissues

Brain tissue samples from human control subjects and demented patients clinically diagnosed as sporadic cases of Alzheimer's disease were dissected at autopsy, fixed in 10% formalin and embedded in paraffin. Samples of frontal cortex and cerebellum were also stored at −80°C. Supplementary Table 1 summarizes the clinical data and the neuropathological staging of control subjects and patients with Alzheimer's disease according to Braak and Braak staging for neurofibrillary tangles (Braak and Braak, 1991) and the Consortium to Establish a Registry for Alzheimer's disease score for senile plaques (Mirra *et al*., 1991). All studies on post-mortem brain tissue were performed in compliance and following approval of the Ethical Committee of the Medical School of the Université Libre de Bruxelles.

Mice

Mice were maintained on a 12-h light/dark cycle, with food and water *ad libitum*. All procedures were approved by the Ethical Committee of the Medical School of the Université Libre de Bruxelles. 2Tg Camk2a-tTA/HA-Itpkb (2Tg) mice are double transgenic mice generated by

Downloaded from https://academic.oup.com/brain/article/137/2/537/283818 by guest on 23 April 2024

crossing the Camk2a-tTA mouse line, which directs the tet-regulatable transcriptional activator (tTA) specifically in forebrain neurons, with the TW2 mouse line (Maréchal *et al*., 2007). The TW2 mouse line contains the TW2 transgene encoding the TetO–hCMV minimal promoter, which requires tTA for its activity, and the mouse haemagglutinin A (HA)-tagged *Itpkb* complementary DNA. '2Tg mut' are double transgenic mice generated by crossing the Camk2a-tTa mouse line with the TM17 mouse line. The TM17 mouse line contains the TM17 transgene encoding the TetO–hCMV minimal promoter and a HA-tagged catalytically-inactive mutant *Itpkb*$^{D743A+K745I}$ complementary DNA. 5xFAD heterozygote mice express five familial Alzheimer's disease (5XFAD) mutations for APP and for PSEN1 (Oakley *et al*., 2006). Mutant APP and PSEN1 transgene expression is driven by the *Thy*1 promoter in these mice. 2Tg 5XFAD and 2Tg mut 5xFAD mice were obtained by crossing the 2Tg or 2Tg mut mice with 5xFAD mice. Genotyping for human APP, HA-*Itpkb* and tTa was performed by PCR amplification as reported (Oakley *et al*., 2006; Maréchal *et al*., 2007). For all experiments, transgenic animals of either sex were compared to age- and background-matched littermate controls.

Cell culture

The mouse Neuro-2a APP$^{K695N+M596L}$ neuroblastoma cell line is a stable N2a clone expressing a myc-tagged FAD Swedish double mutant APP$^{K695N+M596L}$ protein (Thinakaran *et al*., 1996). These cells were maintained in Dulbecco's modified Eagle's medium/Opti-MEM® (0.8:1 v/v), with 200 μg/ml G418 (Life Technologies, Invitrogen), 5% foetal bovine serum, 2 mM L-glutamine, 100 units/ml penicillin, 100 mg/ml streptomycin, and kept at 37°C in humidified 5% CO_2/95% air. The cells were split twice weekly when growing up to 80% confluence. Plasmids used for *Itpkb* overexpression [*Itpkb*, green fluorescent protein (GFP)-*Itpkb*, GFP-*Itpkb*^{D897N}, GFP-*Itpkb*$^{\Delta 1-482}$] in Neuro-2a APP$^{K695N+M596L}$ cells were previously described (Dewaste *et al*., 2003). The GFP plasmid is the pEGFP-C3 expression vector alone (Clontech). The γ-secretase inhibitor DAPT (D5942, Sigma-Aldrich) was used at a concentration of 250 nM. For cell counting, western blotting and amyloid-β_{40} or amyloid-β_{42} peptides ELISA (Biosource, Invitrogen), cells were plated (10^5 cells per well) on a 6-well plate and transfected the day after with 1 μg of plasmid using FuGENE®6 (Roche Applied Science) transfection reagent. In specific experiments, a mitogen-activated protein kinase kinases (MEK) 1/2 inhibitor (Calbiochem SL327; final concentration: 1 μM), dissolved in dimethyl sulphoxide, was added in the culture medium 12 h after cell transfection. Cell supernatant was collected 36 h after transfection, and 1 mM Pefabloc® (Roche Applied Science) was added to prevent amyloid-β peptide degradation. Supernatant was used to quantify extracellular amyloid-β_{40} or amyloid-β_{42} peptides (see below). Cells were harvested, centrifuged, washed in cold PBS and resuspended in PBS, 1% bovine serum albumin and 0.1% sodium azide. Cells were counted on a FC 500 flow cytometer (Beckman Coulter) using size-calibrated fluorescent beads (Flow Count™ Fluorospheres; Beckman-Coulter). For cell viability, apoptosis or proliferation, cells were plated at 4×10^3 cells per well on a 96-well plate and were transfected the following day during 36 h. Cell viability was assessed using Cell Counting Kit-8 assay (Dojindo). Cell Death Detection ELISAPLUS assay and Cell Proliferation ELISA/BrdU colorimetric assay (both from Roche) were used for apoptosis and proliferation assays, respectively. The results of the apoptosis and the proliferation assays were normalized with the results obtained for the viability assay in the same experiment. Primary cultures of cortical neurons were performed using embryonic Day 18 rat forebrains as reported (Morel *et al*., 2010). Cortical astrocytes were prepared from brain of 1-day-old newborn C57BL/6 mice by mechanical dissociation of cortical tissue and seeding of cells on coverslips as described (Macq *et al*., 1998).

Preparation of tissue, cells and brains homogenates

Human frontal cortex and mice brains were homogenized in 5-fold volume of RIPA buffer (Pierce) including protease inhibitors (Complete™, Roche Diagnostics) and phosphatase inhibitor cocktail II (Sigma). The homogenates were rotated at 4°C for 30 min and centrifuged at 13 200*g* for 30 min at 4°C to obtain a pellet P1 and a supernatant S1. For the mice brain homogenates, the pellets P1 containing the amyloid plaques-insoluble material were resuspended in 1-fold volume of formic acid and were rotated at 4°C overnight, neutralized by addition of 19-fold volume of 1 M unbuffered Tris and centrifuged at 1800*g* for 10 min at 4°C to obtain a supernatant S2. S1 and S2 fractions were analysed by western blotting. For soluble APPα and membrane bound APP detection, hemibrains without cerebellum were homogenized in ice-cold buffer (0.02 M Tris–HCl, pH 8.5) containing a protease inhibitor cocktail (Complete Roche) and a phosphatase inhibitor cocktail (Phosphatase Inhibitor Cocktail 2 Sigma), and centrifuged for 1 h at 135 000*g* at 4°C. Supernatant S1 was collected and used for the detection of soluble APPα protein by western blot and ELISA. The pellet fraction containing membrane-bound proteins was resuspended in an ice-cold RIPA buffer with the same protease and phosphatase inhibitor cocktails. After 1 h incubation on ice, it was centrifuged for 15 min at 13 000*g* at 4°C. The supernatants were collected and used for the detection of the membrane-bound APP. The mouse monoclonal antibody 6E10 (Covance) directed against amino-acids 1–16 of human amyloid-β peptide was used for the detection of full-length APP and soluble APPα in their respective fraction. For cells homogenates, cells were collected and lysed in cold RIPA buffer with protease and phosphatase inhibitors. Cell debris was removed and supernatant was collected by high-speed centrifugation at 13 200*g* for 30 min at 4°C. Protein concentrations of the samples were determined by Bradford assay (Bio-Rad). For western blot analysis, 100 or 200 μg of total protein was resolved by 8%, 10% or 16% SDS-PAGE (Bio-Rad), blotted onto nitrocellulose or polyvinylidene difluoride membranes. The membranes were blocked in semi-fat dry milk (10% w/v in Tris-buffered saline) for 1 h at room temperature and overnight incubated with the appropriate primary antibody. For the enhanced chemiluminescent revelation, the membranes were then incubated with a horseradish peroxidase-conjugated secondary antibody [goat anti-rabbit (A4914, Sigma-Aldrich) or horse anti-mouse (Vector Laboratories)]. Finally, the peroxidase activity was detected with the enhanced chemiluminescent detection kit and visualized with CL-XPosure Film (Thermo Scientific). For the nitro-blue tetrazolium/5-bromo-4-chloro-3′-indolyphosphate revelation method, the nitrocellulose sheets were then incubated with anti-rabbit or anti-mouse immunoglobulins conjugated to alkaline phosphatase (Sigma-Aldrich). Finally, the membranes were incubated in developing buffer (0.1 mol/l Tris, 0.1 mol/l NaCl, 0.05 mol/l $MgCl_2$; pH 9.5) containing nitro-blue tetrazolium/5-bromo-4-chloro-3′-indolyphosphate (Pierce). The reaction was stopped by dipping the membranes in 10 mmol/l Tris, 1 mmol/l ethylenediaminetetraacetic acid (pH 8). The western blot quantification was achieved by densitometry analysis of each band using Image J software (NIH) and normalized for protein loading based on the anti-actin or anti-tubulin signals.

Downloaded from https://academic.oup.com/brain/article/137/2/537/283818 by guest on 23 April 2024

Amyloid-β and soluble APPα ELISAs BACE1 activity test

S1, S2 and culture medium of Neuro-2a $APP^{K695N+M596L}$ transfected cells were analysed by ELISA to determine the production of amyloid-β_{40} and amyloid-β_{42} peptides (Biosource, Invitrogen), as well as of soluble APPα (FIVEphoton Biochemicals). Amyloid-β_{40} and amyloid-β_{42} concentrations were determined by comparison with the amyloid-β_{40} and amyloid-β_{42} standard curves. S1 was used to perform the BACE1 activity assay (SensiZyme BACE1 Activity Assay Kit, Sigma-Aldrich).

Immunohistochemistry

Transfected Neuro-2a $APP^{K695N+M596L}$ cells and primary cultures were cultured on sterile glass coverslips and fixed for 15 min in 4% (w/v) paraformaldehyde and 4% (w/v) sucrose in 0.1 M phosphate buffer. Before immunolabelling, fixed cultures were treated for 5 min with 0.01 M Tris, 0.15 M NaCl, pH 7.6 containing 0.3% (w/v) Triton™ X-100. Brains were fixed in 10% formalin for 24 h before embedding in paraffin and 7-µm thick tissue sections performed in the sagittal plane. The immunohistochemical labelling was performed using the ABC method. Briefly, formalin-fixed tissue sections embedded in paraffin (7-µm thick) were treated with H_2O_2 to inhibit endogenous peroxidase and incubated with the blocking solution [10% (v/v) normal serum; normal horse serum for mouse monoclonal primary antibodies and normal goat serum for rabbit polyclonal primary antibodies]. After an overnight incubation with the primary antibody, the sections were sequentially incubated with secondary antibody conjugated to biotin (horse anti-mouse antibody for monoclonal primary antibody and goat anti-rabbit antibody for rabbit polyclonal primary antibody; Vector Laboratories) before the ABC complex (Vector). The peroxidase activity was revealed using diaminobenzidine as chromogen. For immunolabelling of the amyloid-β antibodies, rehydrated tissue sections were pretreated with 100% formic acid for 10 min before incubation with the blocking solution. Tissue sections were examined with a Zeiss Axioplan I microscope (Carl Zeiss) and digital images acquired using an Axiocam HRc camera (Carl Zeiss). Double immunolabelling was performed using fluorescent markers. The first primary antibody was detected using FITC-conjugated antibody (Jackson) and the second primary antibody was detected using a biotinylated antibody, followed by streptavidin conjugated to Alexa Fluor® 594 (Molecular Probes). For Congo Red staining, brain sections were first stained with Mayer's haematoxylin solution and incubated in alkaline sodium chloride solution. Sections were then stained with alkaline Congo Red solution (0.2% in 80% ethanol saturated with sodium chloride) and washed in absolute ethanol. For Nissl staining, brain sections were counterstained with the Nissl method to stain Nissl substance in neurons. Hydrated tissue sections were stained for 20 min with Cresyl violet [0.1 % (w/v) in acetic acid/sodium acetate solution] and differentiated into 70 % (v/v) and 90% (v/v) alcohol, before dehydratation and mounting.

For quantification of amyloid-β load on tissue sections, mouse sagittal brain sections were immunolabelled with the amyloid-β_{40} or amyloid-β_{42} antibody according to the ABC method. Digital images covering the whole hemisphere were acquired with a ×2.5 objective lens and a camera (CX9000) mounted on a motorized Zeiss AxioimagerM1 microscope (Carl Zeiss) and the virtual slice module of StereoInvestigator (MicroBrightField) software, as reported. The total cortex surface was measured using manual selection and the amyloid-β immunolabelled area in the cortex was determined with the ImageJ program (NIH) by detecting positive pixels using image thresholding, as reported (Leroy *et al*., 2012). The area covered by amyloid-β deposits was expressed relatively to the total cortex surface.

Quantitative polymerase chain reaction

Brains of 5XFAD mice were homogenized with a teflon/glass homogenizer and total RNA was extracted using TriPure lysis solution and High Pure RNA Tissue Kit (Roche Diagnostics) according to the manufacturer's protocol, which included DNase treatment. One microgram of total RNA was reverse-transcribed into complementary DNA with SuperScript® II enzyme, oligo(dT), dNTP mix, First-Strand Buffer, DTT, RnaseOUT (Invitrogen). The messenger RNA quantification was performed using a real-time PCR on a LightCycler 480. Primers sequences [β-actin sense, 5′-TCC-TGA-GCG-CAA-GTA-CTC-TGT-3′; β-actin antisense, 5′-CTG-ATC-CAC-ATC-TGC-TGG-AAG-3′; β-actin probe, 5′-(6-Fam)ATC-GGT-GGC-TCC-ATC-CTG-GC-3′ (Tamra) (phosphate); *Itpkb* sense, 5′-GCT-TTC-AGA-GAA-TTC-ACT-AAG-GGA-A-3′; *Itpkb* antisense, 5′-CTT-CTT-CAA-GTG-CCA-CGA-GGT-3′; *Itpkb* probe, 5′-(6-Fam)CTG-AAG-GCC-ATT-CGA-GCG-ACC-CT-3′ (Tamra); hypoxanthine-guanine phosphoribosyltransferase (*Hprt*) sense 5′-GGA-CCT-CTC-GAA-GTG-TTG-GAT-3′, *Hprt* antisense 5′-CCA-ACA-ACA-A AC-TTG-TCT-GGA-A-3′; and *Hprt* probe 5′-(6-Fam)CAG-GCC-AGA-CTT-TTG-TTG-GAT-TTG-AA-3′ (Tamra)] were designed with Primer3 software (Whitehead Institute for Biomedical Research). Quantitative PCR was achieved using commercial kit LightCycler® TaqMan® Master (Roche) and cycling programme was 5 min at 95°C and then 40 cycles, each consisting of 15 s at 95°C, and 30 s at 60°C. According to the delta delta Ct method, gene expression level of each messenger RNA was calculated in duplicate, further normalized to actin or *Hprt* messenger RNA and related to control mice.

Antibodies

ITPKA and ITPKB antibodies are rabbit polyclonal antibodies (Takazawa *et al*., 1990; Hascakova-Bartova *et al*., 2004). The total tau (B19) antibody is a rabbit polyclonal antibody raised to adult bovine tau proteins, reacting with all adult and foetal tau isoforms in bovine, rat, mouse, and human nervous tissue in a phosphorylation-independent manner. The mouse monoclonal antibodies PHF-1 and CP13 (kindly provided by Drs P. Davies and S. Greenberg, New York, NY) are specific for tau phosphorylated at Ser396/404 and Ser202/Thr205, respectively. The following additional antibodies were also used: rabbit polyclonal antibodies specific for phospho Ser262 tau (BioSource, Invitrogen), ERK1/2 and phosphoERK1/2 (Cell signalling), total amyloid-β (Aβ1–12, Dako), amyloid-β_{42} (Millipore) amyloid-β_{40} (Biosource, Invitrogen), MAP2 B9 antibody (Brion *et al*., 1988), GFP (Molecular Probes). The mouse monoclonal antibodies to α-tubulin (clone DM1-A) and to GFAP (clone GA5) and the rabbit polyclonal antibodies to HA epitope and to actin were from Sigma. 6E10, a mouse monoclonal antibody to residues 1–16 of amyloid-β, was from Signet (Dedham). The mouse monoclonal antibody specific for the Golgi matrix protein of 130 kDa (GM 130) was from BD Transduction Laboratories.

Inositol 1,3,4,5-tetrakisphosphate level

Neuro-2a $APP^{K695N+M596L}$ cells were grown in 10 cm culture dish to 80% confluency, harvested and resuspended in 3 ml of medium; 1 ml was used for plating in antibiotic-free medium containing 20 µCi/ml of ^{3}H-Inositol 1 day before transfection. Cells were transfected with indicated constructs and harvested 12 h later. Inositol phosphates were extracted and analysed by high-performance liquid chromatography

Downloaded from https://academic.oup.com/brain/article/137/2/537/283818 by guest on 23 April 2024

(Jia *et al*., 2007). Before extraction of inositol phosphate, a fraction of cell suspension was taken and lysed for protein level determination. Inositol phosphate levels were normalized to protein level and transfection efficiency in total cells. Transfection efficiency was determined by analysing GFP fluorescence 1 day after transfection. Data were from three independent assays performed in duplicate.

Statistical analysis

All values are expressed as means ± standard error of the mean (SEM). Significance of differences between two means was calculated using the GraphPad InStat software (GraphPad Software). Statistical comparisons were performed using one-way analysis of variance with Bonferroni *post hoc* test comparisons, unpaired two-tailed Student's *t*-test or Mann-Whitney test (non-parametric tests algorithms). The significance level of the differences of the means (*P*-value) is indicated in the legend of each figure.

Results

ITPKB protein expression and localization in the cerebral cortex of patients with Alzheimer's disease and in the 5XFAD transgenic mouse model

The expression and localization of the ITPKB protein were first analysed by immunohistochemistry on tissue sections from the frontal cortex of control human subjects and from wild-type mouse brain (Supplementary Fig. 1A and Supplementary Table 1 for information on control subjects and patients with Alzheimer's disease). Both human and mouse cortical neurons and astrocytes were labelled with the ITPKB antibody. This cellular localization was also observed in primary cultures of mouse embryonic cortical neurons and astrocytes (Supplementary Fig. 1B–D). Next, the level of ITPKB protein was quantified in frontal cortex homogenates from 14 patients with sporadic Alzheimer's disease and nine control subjects (Fig. 1A and B and Supplementary Table 1). A ~3-fold increase in ITPKB protein level was detected in most patients with Alzheimer's disease, as compared with control subjects. Indeed, when normalized to actin [control: 0.288 ± 0.072 arbitrary units (AU); Alzheimer: 0.739 ± 0.091 AU; $P = 0.002$, Student's *t*-test], the mean ITPKB protein level was significantly higher in the Alzheimer group than in the control group (Fig. 1B). ITPKB level was also significantly higher in the Alzheimer group after normalization with GFAP (control: 0.056 ± 0.010 AU; Alzheimer: 0.219 ± 0.041 AU; $P = 0.004$, Student's *t*-test), indicating that it did not result simply from increased astrocytosis in the Alzheimer's disease brain. By contrast, the mean level of ITPKA, the major ITPK isoform expressed in brain, was similar in the frontal cortex of patients with Alzheimer's disease and control subjects (control: 0.441 ± 0.084 AU; Alzheimer's disease: 0.315 ± 0.045 AU; $P = 0.214$, Student's *t*-test; Fig. 1A and B), as was the ITPKB level in the cerebellum (data not shown). The post-mortem interval did not influence the detection levels of ITPKB protein, as there was no significant correlation between these two variables in the control group (Pearson $r = 0.2696$, $P = 0.52$, two-tailed), in the Alzheimer's disease group (Pearson $r = 0.0077$, $P = 0.98$, two-tailed), or after grouping them together (Pearson $r = 0.0828$, $P = 0.71$, two-tailed). Double immunolabelling on frontal cortex sections from patients with Alzheimer's disease showed that the strongest ITPKB immunoreactivity was localized in dystrophic neurites associated with amyloid plaques (Fig. 1C and Supplementary Fig. 2A). By contrast, ITPKB immunoreactivity in astrocytes was similar in the frontal cortex of patients with Alzheimer's disease and control subjects (data not shown). No ITPKB immunoreactivity was associated with intracellular neurofibrillary tangles (data not shown). ITPKB protein expression and localization were next analysed in a transgenic mouse model of Alzheimer's disease: the 5XFAD mouse (Oakley *et al*., 2006). This transgenic mouse expresses familial Alzheimer's disease mutant APP and PSEN1, produces high levels of amyloid-β peptides and rapidly develops amyloid plaque pathology and impaired memory similar to that found in patients with Alzheimer's disease (Oakley *et al*., 2006). ITPKB protein level was not significantly different in the cortex of 6-month-old control and 5XFAD transgenic mice (control: 0.60 ± 0.17 AU; 5XFAD: 0.53 ± 0.09 AU), as found in a minority of patients with Alzheimer's disease (Fig. 1D). Similarly to what we previously observed in tissue from patients with Alzheimer's disease, the mouse ITPKB protein was also accumulated in dystrophic neurites associated with amyloid plaques (Fig. 1E and Supplementary Fig. 2B). ITPKB levels were not significantly different in the cortex of 1-month-old control and 5XFAD mice, i.e. before the appearance of amyloid-β deposits (control: 0.70 ± 0.02 AU; 5XFAD: 0.65 ± 0.03 AU).

These results indicate that the level of ITPKB protein is higher in the frontal cortex of most patients with Alzheimer's disease; they also highlight the striking neuritic accumulation of ITPKB around extracellular deposits of amyloid-β peptides in patients with Alzheimer's disease and in 5XFAD transgenic mice.

Apoptosis and altered APP metabolism in Neuro-2a APP cells overexpressing ITPKB protein

As the level of ITPKB was higher in most patients with Alzheimer's disease and ITPKB was abundant in dystrophic neurites around amyloid deposits, the effect of ITPKB overexpression was investigated in a neuronal cell line. Mouse Neuro-2a neuroblastoma cells expressing a myc-tagged FAD Swedish double mutant $APP^{K695N+M596L}$ protein were used for transfection studies (Thinakaran *et al*., 1996). In *Itpkb*-transfected cells, a ~6-fold increase in ITPKB protein (non-transfected cells: 0.54 ± 0.09 AU; *Itpkb*-transfected cells: 3.18 ± 0.21 AU) and a ~2.5-fold increase in Ins(1,3,4,5)P4 level ($P = 0.05$) were observed, as compared with non-transfected cells (Supplementary Fig. 3). Surprisingly, compared with GFP-transfected cells, expression of the ITPKB protein or the GFP-ITPKB fusion protein was associated with markedly lower cell counts 36 h after transfection (Fig. 2A). Expression of a catalytically-inactive ITPKB mutant protein (GFP-$ITPKB^{D897N}$) (Dewaste *et al*., 2003) yielded similar results, indicating that Ins(1,3,4,5)P4 production was not essential for this effect (Fig. 2A). By contrast, the effect on cell count was not observed

Downloaded from https://academic.oup.com/brain/article/137/2/537/283818 by guest on 23 April 2024

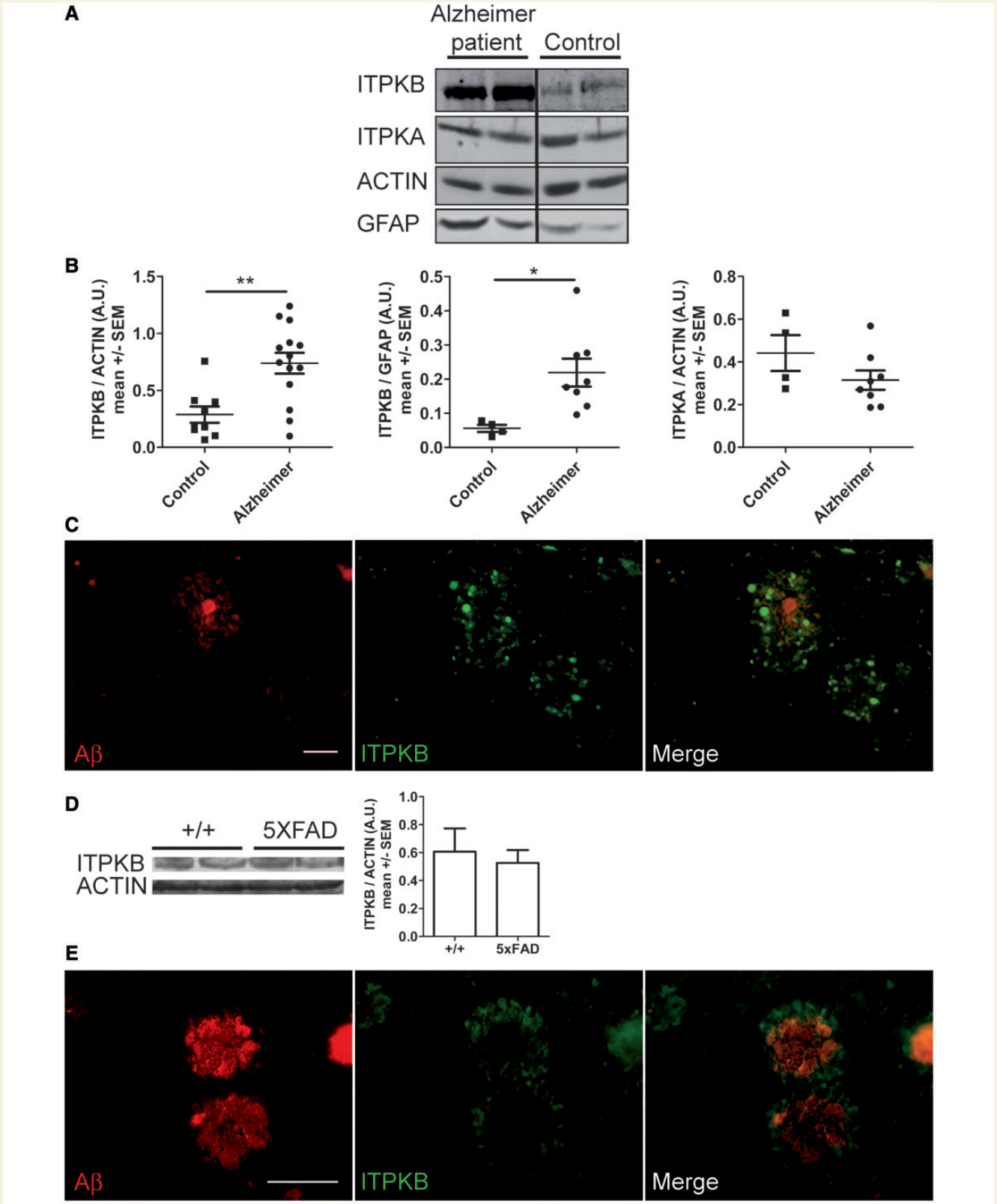

Figure 1 Higher ITPKB expression in the cortex of patients with Alzheimer's disease and accumulation in dystrophic neurites around amyloid deposits in human patients with Alzheimer's disease and 5XFAD transgenic mice. (**A**) Immunoblot analysis for ITPKB and ITPKA expression in frontal cortex homogenates isolated from 8–14 patients with sporadic Alzheimer's disease and four to nine control subjects. Actin and GFAP were used as a loading control. (**B**) Quantification of the 110 kDa ITPKB and the 50 kDa ITPKA signals obtained in (**A**): the ITPKB/ACTIN and ITPKB/GFAP signals ratio are significantly higher for patients with Alzheimer's disease than for control subjects. No difference is observed for the ITPKA/ACTIN signals ratio. $*P < 0.05$, and $**P < 0.01$ by Student's *t*-test. (**C**) Immunofluorescence studies

(continued)

Downloaded from https://academic.oup.com/brain/article/137/2/537/283818 by guest on 23 April 2024

after deletion of the first 482 amino acids of ITPKB, which are known to be important for correct subcellular localization of the protein (Fig. 2A) (Dewaste *et al*., 2003). Similar results, although quantitatively less marked, were obtained after transfection of Neuro-2a cells, which do not express exogenous human APP (data not shown). Decreased Neuro-2a $APP^{K695N+M596L}$ cell count after GFP-ITPKB transfection was associated with a decrease in cell viability and a significant increase in cell apoptosis, but without evident alteration in cell proliferation (Fig. 2B). No difference in cell viability, apoptosis or proliferation was observed between cells transfected with GFP and with the N-terminal GFP-$ITPKB^{\Delta 1-482}$ deletion mutant (Fig. 2B). Interestingly, amyloid-β_{40} and amyloid-β_{42} peptides levels were significantly higher in the culture medium of Neuro-2a $APP^{K695N+M596L}$ cells transfected with GFP-ITPKB than after transfection with GFP (Fig. 2C). Compared with GFP-ITPKB, transfection with GFP-$ITPKB^{D897N}$ or GFP-$ITPKB^{\Delta 1-482}$ mutants led to lower production of amyloid-β peptides, not significantly different from those observed with GFP (Fig. 2C). For the N-terminal ITPKB deletion mutant, GFP-$ITPKB^{\Delta 1-482}$, the absence of amyloid-β peptide overproduction was associated with an altered subcellular localization and an absence of co-localization with APP in the Golgi apparatus (Supplementary Fig. 4). Addition of a MEK1/2 inhibitor to the culture medium completely prevented overproduction of amyloid-β peptides in GFP-*Itpkb* transfected cells, but had no effect on cell survival (Fig. 2D). Production of amyloid-β peptides was not increased after transfection with the GFP-*Itpka* vector (data not shown). Myc-APP metabolism was investigated in Neuro-2a $APP^{K695N+M596L}$ cells transfected with GFP or GFP-*Itpkb*. The myc antibody revealed a significant decrease in APP levels and a significant increase in the β-carboxy terminal fragment (β-CTF)/α-CTF ratio in lysates of GFP-*Itpkb* transfected cell, as compared with GFP, suggesting that APP amyloidogenic processing was enhanced when ITPKB is overexpressed (Fig. 2E). The significantly increased BACE1 activity observed in GFP-*Itpkb* transfected cells, as compared with GFP, confirmed this hypothesis and was associated with a normal α-secretases activity (Fig. 2F).

Taken together, our results in Neuro-2a $APP^{K695N+M596L}$ cells indicate that ITPKB overexpression leads to increased cell apoptosis, BACE1 activity and production of amyloid-β peptides. Reducing production of amyloid-β peptides with the γ-secretase inhibitor DAPT had no significant influence on cell apoptosis induced by ITPKB overexpression, suggesting that apoptosis is not the direct consequence of overproduction of amyloid-β peptides in this cellular model (data not shown). Production of Ins(1,3,4,5)P4 by overexpressed ITPKB must take place at specific subcellular sites, may be close to APP in the Golgi apparatus, to induce overproduction of amyloid-β peptides in Neuro-2a $APP^{K695N+M596L}$ cells. Our results also indicate that, like in T and B lymphocytes, the MEK/ERK signalling pathway seems to play an important role downstream of Ins(1,3,4,5)P4 in this effect.

Absence of amyloid plaques and normal phospho-tau protein level in transgenic mice overexpressing the ITPKB protein in neurons:

To investigate the effects of neuronal ITPKB protein overexpression *in vivo*, a double transgenic mouse model named 2Tg Camk2a-tTA/HA-*Itpkb* (or 2Tg) was developed where expression of the HA-tagged *Itpkb* complementary DNA is directed in forebrain neurons by the tetracycline-controlled tTA transactivator (Fig. 3A). As expected, ITPKB protein level was significantly enhanced in cortex and hippocampus neurons of these mice (Fig. 3B–D). Amyloid plaque and tau protein hyperphosphorylation (ratio p-tau $Ser^{396/404}$/tau: +/+: 0.440 ± 0.260 AU; 2Tg: 0.400 ± 0.244 AU) were not observed in the cerebral cortex of 2Tg mice (Fig. 3E and F).

Altogether, these *in vivo* results indicate that ITPKB protein overexpression in forebrain neurons is not sufficient to induce Alzheimer's disease pathology in mice.

Exacerbated Alzheimer's disease pathology in 5XFAD transgenic mice overexpressing ITPKB protein in neurons

As 5XFAD mice do not overexpress the ITPKB protein in the cerebral cortex (Fig. 1D), this Alzheimer mouse model represents an ideal tool to mimic the enhanced ITPKB protein levels observed in most patients with Alzheimer's disease analysed and to investigate its specific consequence(s) on Alzheimer's disease pathology. To this end, we generated a transgenic mouse model named 2Tg Camk2a-tTA/HA-*Itpkb* 5XFAD (or 2Tg 5XFAD) where expression of the HA-tagged *Itpkb* complementary DNA is directed in forebrain neurons of 5XFAD mice by the tetracycline-controlled tTA transactivator.

As expected, the total ITPKB protein level was increased in neurons of 2Tg 5XFAD mice in the cerebral cortex and the hippocampus, as compared with 5XFAD mice (Fig. 4A). The presence of the transgenic APP protein was also confirmed in these mice in the

Figure 1 Continued
on frontal cortex sections from a patient with Alzheimer's disease with antibodies directed against amyloid-β peptides (red, *left*) and ITPKB (green, *middle*): dystrophic neurites around amyloid deposits are strongly ITPKB-positive (*right*). Scale bar = 50 μm. (**D**) Immunoblot analysis for ITPKB expression in cortex homogenates from 6-month-old control ($n = 4$) and 5XFAD ($n = 5$) mice. Actin was used as a loading control. The quantification of the 110 kDa ITPKB signal did not reveal a significant difference with Mann–Whitney test between control (+/+) and 5XFAD mice. (**E**) Immunofluorescence studies on cortex sections from a 6-month-old 5XFAD transgenic mouse with antibodies directed against amyloid-β peptides (red, *left*) and the ITPKB protein (green, *middle*): dystrophic neurites around amyloid deposits are strongly ITPKB-positive (*right*). Scale bars = 50 μm.

Downloaded from https://academic.oup.com/brain/article/137/2/537/283818 by guest on 23 April 2024

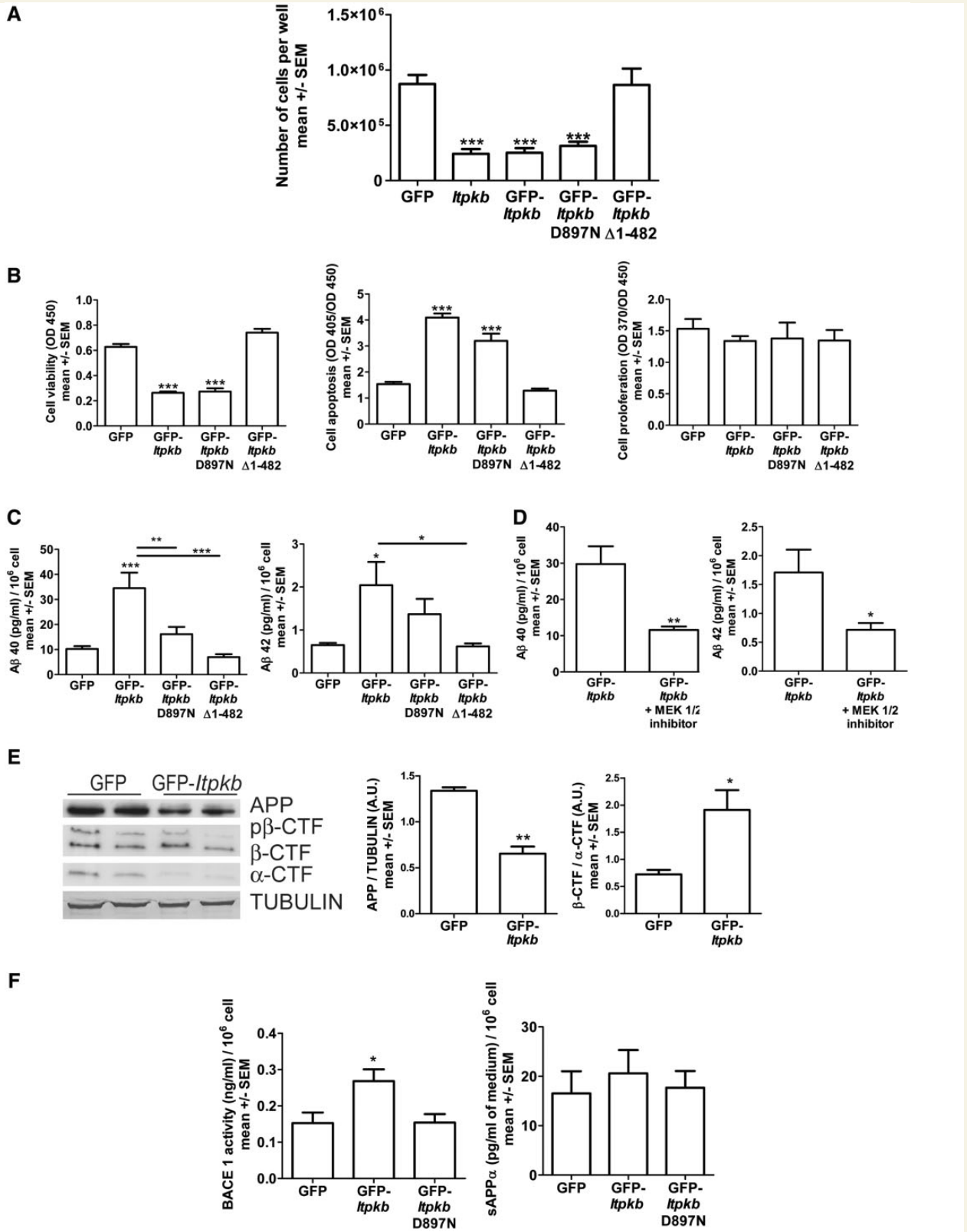

Figure 2 Increased apoptosis and amyloid-β production in Neuro-2a APP$^{K695N+M596L}$ cells overexpressing ITPKB. Neuro-2a APP$^{K695N+M596L}$ cells were transfected with plasmids expressing GFP, ITPKB, GFP-ITPKB, GFP-ITPKB^{D897N} or GFP-ITPKB$^{\Delta 1-482}$ proteins and analysed 36 h later. Between 60% and 80% of cells were GFP positive by flow cytometry analysis after transfection with GFP-expressing plasmids. In specific experiments, GFP-*Itpkb* transfected cells were incubated with a MEK1/2 inhibitor (final concentration: 1 μM) or with dimethyl sulphoxide-containing solvent. No significant difference was observed between GFP-*Itpkb* transfected cells without and with dimethyl sulphoxide (data not shown). (**A**) Cell counts per 10 cm^2 well using fluorospheres and flow cytometry. Results

(continued)

Downloaded from https://academic.oup.com/brain/article/137/2/537/283818 by guest on 23 April 2024

same brain regions. Levels of human mutant APP and PSEN1 were not significantly different between 5XFAD mice and 2Tg 5XFAD mice (Figs 4B and 5C and data not shown). An increased number of GFAP positive astrocytes was observed in the cortex of 2Tg 5XFAD mice compared with 5XFAD mice, indicating that increased ITPKB expression in neurons induced astrogliosis (Fig. 4C). The more severe astrogliosis in 2Tg 5XFAD mice was confirmed by the presence of an increased level of GFAP detected by western blotting in brain homogenates of these mice, as compared with 5XFAD mice (Supplementary Fig. 5). Amyloid plaques were present at a higher density in the cortex of 2Tg 5XFAD mice than in 5XFAD mice; interestingly, amyloid-β_{40} and amyloid-β_{42} peptide-specific antibodies revealed that only amyloid-β_{40} immunoreactivity was increased in the cortex of 2Tg 5XFAD mice (Fig. 5A). This result was confirmed by the quantification of amyloid-β_{40} and amyloid-β_{42} plaque surface in the cortex of 2Tg 5XFAD and 5XFAD mice (Fig. 5A), and by quantification of amyloid-β_{40} and amyloid-β_{42} peptides in the insoluble fraction of brain homogenates from the same mice (Fig. 5B). Compared with 5XFAD mice, a significantly increased level of β-CTF signal was detected in brain homogenates of 2Tg 5XFAD mice, suggesting that APP processing was altered in these latter mice by shifting towards the amyloidogenic pathway, as observed in Neuro-2a $APP^{K695N+M596L}$ cells overexpressing ITPKB (Fig. 5C). The increased β-CTF signal in 2Tg 5XFAD brain homogenates was associated with a significantly increased BACE1 activity (Fig. 5D) and a normal α-secretase activity (Fig. 5E), as in Neuro-2a $APP^{K695N+M596L}$ cell transfection studies. Surprisingly, in brain homogenates from 2Tg 5XFAD mice, tau proteins were significantly hyperphosphorylated at $Ser^{396/404}$ and Ser^{202}, as compared with 5XFAD mice (Fig. 6A). Phosphorylation of tau proteins on some sites decreases their electrophoretic mobility, and phosphorylated tau species with apparent higher molecular weight were also detected and more abundant in 2Tg 5XFAD brain (Fig. 6A). Gallyas staining did not identify neurofibrillary tangles in 2Tg 5XFAD mice (data not shown).

Mechanistically, Alzheimer pathology exacerbation in 6-month-old 2Tg 5XFAD brain was associated with an increased activating phosphorylation of ERK1/2, as compared with 5XFAD mice (Fig. 6B). No increased phosphorylation of ERK1/2 was observed in 5XFAD mice at 1 month, as compared with control mice (pERK1/2/ERK1/2: control mice: 0.53 ± 0.16 AU; 5XFAD mice: 0.84 ± 0.17 AU; $P = 0.285$ by Mann–Whitney test). The specific role of ITPKB-produced Ins(1,3,4,5)P4 was investigated *in vivo* by expression of a catalytically-inactive mutant HA-$ITPKB^{D743A+K745I}$ protein in forebrain neurons of 5XFAD mice (Supplementary Fig. 6). In these transgenic mice named 2Tg mut 5XFAD mice, Alzheimer's disease pathology was similar as in 5XFAD mice. Indeed, amyloid plaques area, β-CTF levels and tau protein phosphorylation were similar in these mice and in 5XFAD mice (Supplementary Fig. 6).

Altogether, these *in vivo* results indicate that ITPKB protein overexpression in forebrain neurons of an APP/PSEN1 mouse model exacerbates Alzheimer's disease pathology: amyloid-β_{40} amyloid plaques surface, amyloid-β_{40} peptide production, tau phosphorylation and astrogliosis were significantly increased when the ITPKB protein was overexpressed. This Alzheimer's disease pathology exacerbation was dependent on the production of Ins(1,3,4,5)P4 by the overexpressed transgenic ITPKB protein and was associated with increased ERK kinases activation and BACE1 activity.

Discussion

We report here that a majority of patients with Alzheimer's disease tested in our study overexpress the ITPKB protein in the cerebral cortex, and that neuronal ITPKB protein overexpression is associated with increased cell death, enhanced astrogliosis, production of amyloid-β peptides and amyloid plaque formation as well as with increased tau phosphorylation in an Alzheimer's disease mouse model. Thus, our results first extend to the protein level published data about the *ITPKB* messenger RNA overexpression detected by microarray analysis on a large cohort of patients with Alzheimer's disease (Emilsson *et al*., 2006). Second, they highlight that ITPKB and Ins(1,3,4,5)P4 are important regulators of Alzheimer's disease pathology *in vivo*. Third, they indicate that,

Figure 2 Continued
are representative of four independent experiments, $n = 6$ for each experiment. $***P < 0.001$ by one-way ANOVA (Bonferroni's multiple comparison test). (**B**) Cell viability [WST-8 tetrazolium salt cleavage assay; expressed as optical density (OD) at 450 nm; *left*], apoptosis (histone-complexed DNA fragments assay on cells, relative to cell viability; expressed as OD at 405/450 nm; *middle*) and proliferation (BrdU DNA incorporation assay, relative to cell viability; expressed as OD at 370/450 nm; *right*) were determined by colorimetric assays. Results are representative of two independent experiments, $n = 6$ for each experiment. $***P < 0.001$ by one-way ANOVA (Bonferroni's multiple comparison test). (**C** and **D**) Amyloid-β_{40} and amyloid-β_{42} peptide concentrations were determined in the culture medium of transfected cells by ELISA. Results are expressed as mean ± SEM of pg/ml of peptides produced by 10^6 cells. Results are representative of two or three independent experiments, $n = 6$ for each experiment. $*P < 0.05$, $**P < 0.01$ and $***P < 0.001$ by one-way ANOVA (Bonferroni's multiple comparison test) (**C**) or by Student's *t*-test (**D**). (**E**) APP metabolism analysis in GFP and GFP-*Itpkb* transfected cells by immunodetection with a myc antibody. A tubulin antibody was used as loading control. APP was quantified relative to tubulin and the β-CTF/α-CTF ratio was determined. Similar results were obtained in independent experiments with an antibody directed to the 17 APP-carboxy terminus amino acids (data not shown). $*P < 0.05$, and $**P < 0.01$ by Student's *t*-test. (**F**) BACE1 activity was analysed by ELISA in homogenates of GFP, GFP-*Itpkb* and GFP-$Itpkb^{D897N}$ transfected cells. Results are expressed as mean ± SEM of ng/ml of BACE1 produced by 10^6 cells, $n = 6$ for each condition. $*P < 0.05$ by one-way ANOVA (Bonferroni's multiple comparison test). Soluble APPα concentrations were determined in the culture medium of GFP, GFP-*Itpkb* and GFP-$Itpkb^{D897N}$ transfected cells by ELISA. Results are expressed as mean ± SEM of pg/ml of soluble APPα produced by 10^6 cells, $n = 8$ for each condition.

Downloaded from https://academic.oup.com/brain/article/137/2/537/283818 by guest on 23 April 2024

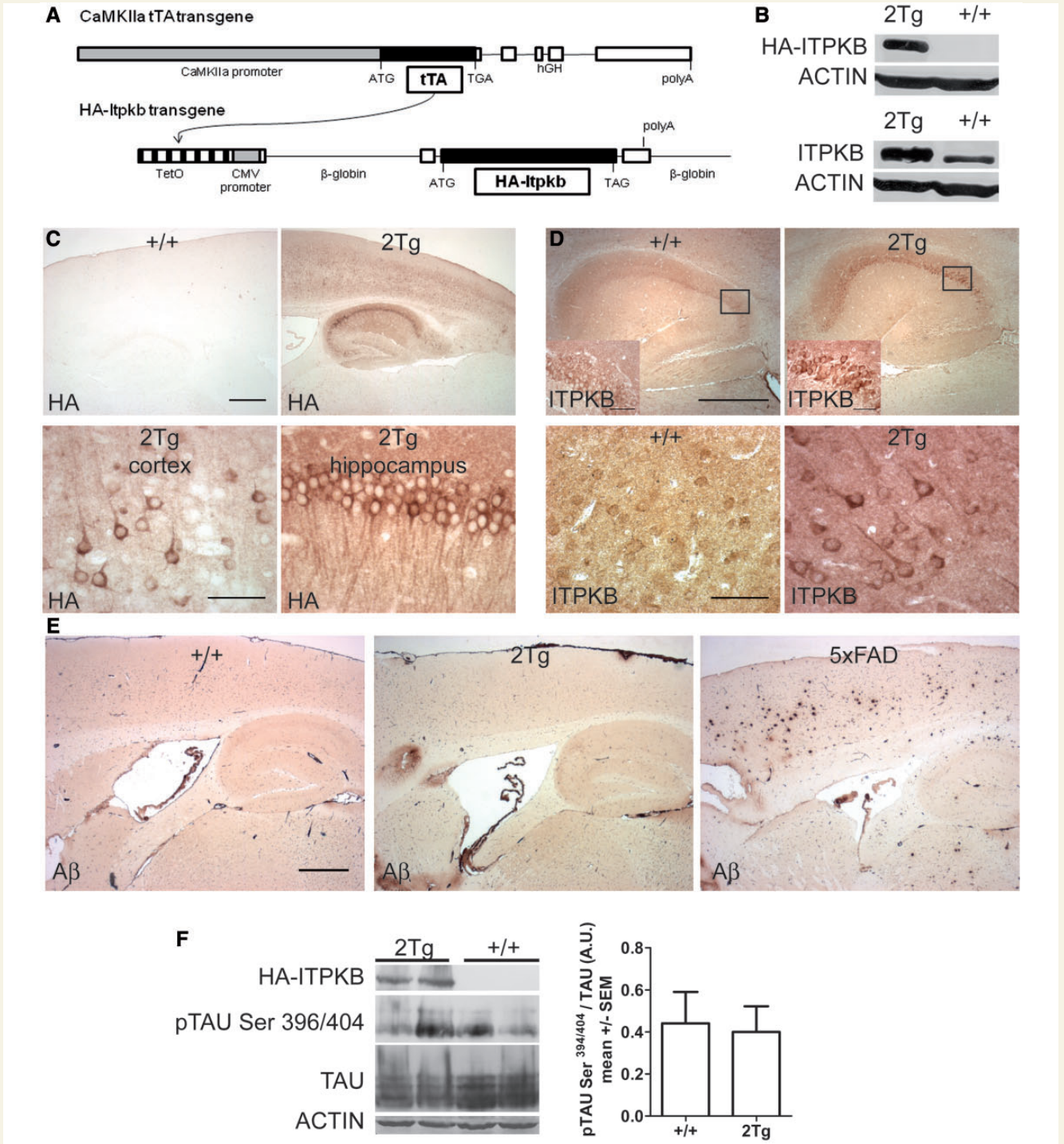

Figure 3 A transgenic mouse that overexpresses ITPKB protein in neurons. (**A**) Camk2a-tTA and HA-*Itpkb* transgenes used to construct the 2Tg Camk2a-tTA/HA-Itpkb mouse (or 2Tg mouse). (**B**) Immunodetection of transgenic HA-ITPKB (*top*) and total ITPKB (*bottom*) proteins in brain homogenates of 6-week-old 2Tg and control (+/+) mice with an HA and an ITPKB antibody, respectively. Actin served as loading control. (**C**) Neuronal localization of the transgenic HA-ITPKB protein in the cortex and the hippocampus of 6-week-old 2Tg mice. *Top*: brain sections of control (+/+) and 2Tg mice were stained with a HA antibody. *Bottom* panels: higher magnifications on neurons from 2Tg cortex (*left*) and 2Tg CA1 region of the hippocampus (*right*). Scale bars = 50 μm. (**D**) Immunodetection with an ITPKB antibody showing the neuronal overexpression of the ITPKB protein in the hippocampus (*top* panels) and the cortex (*bottom* panels) of 6-week-old control (+/+) mice (*left*) and 2Tg mice (*right*). The insets show a higher magnification of the framed part of the brain section. Scale bars = 500 μm (*top*) and 50 μm (*bottom*). (**E**) Immunodetection with an amyloid-β peptide antibody on cortex sections from 6-month-old control (+/+) and 2Tg mice. 5XFAD mice served as positive controls (*right*). Scale bars = 500 μm. (**F**) Immunodetection of tau protein phosphorylated at $Ser^{396/404,}$ tau protein and HA-ITPKB protein in cortex homogenates from 6-month-old control (+/+) and 2Tg mice (*left*). The graph represents the ratio of phosphorylated tau protein relative to total tau protein (*right*) in brain homogenates of four 2Tg and three control mice.

Downloaded from https://academic.oup.com/brain/article/137/2/537/283818 by guest on 23 April 2024

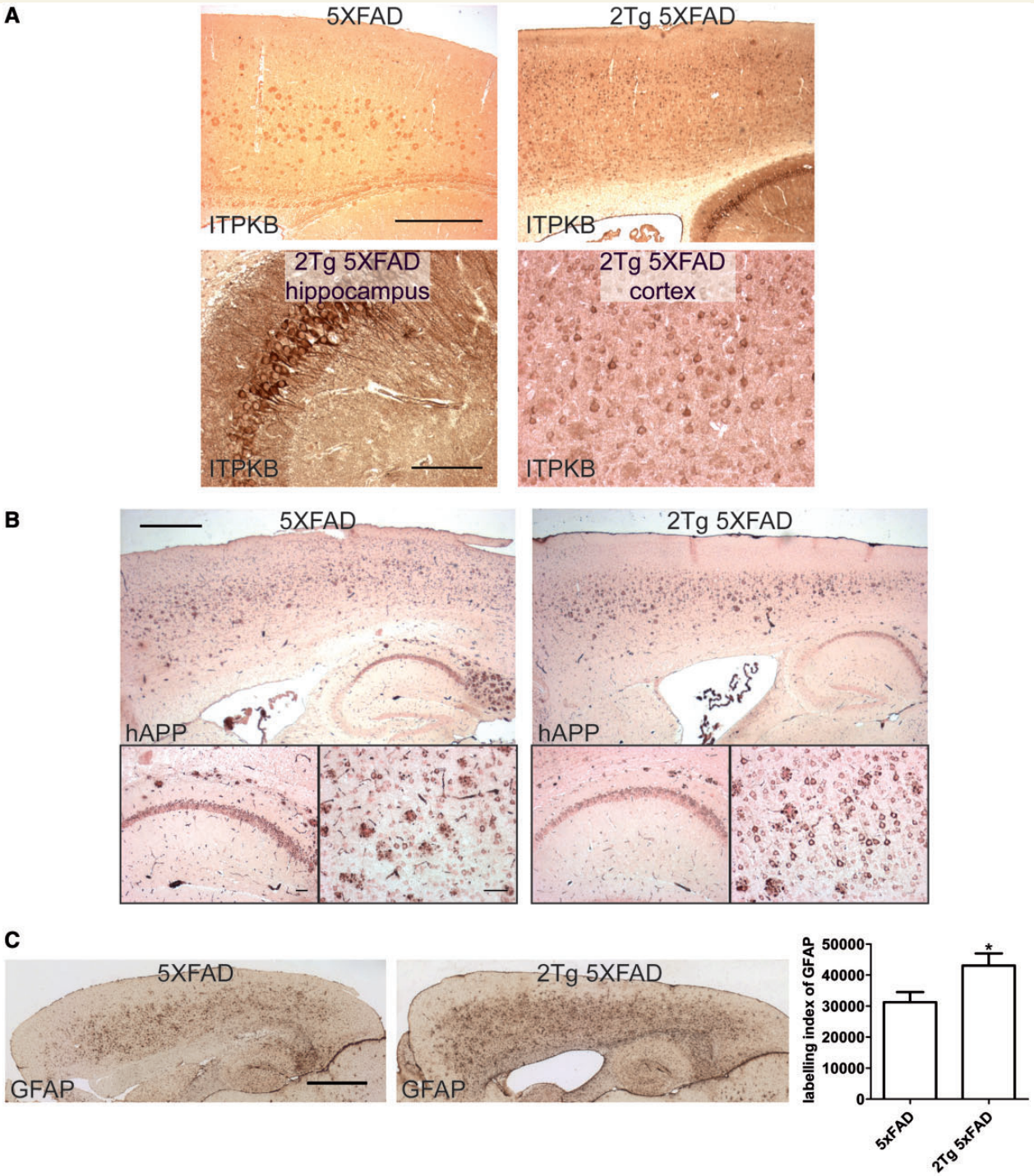

Figure 4 Increased astrogliosis in 5XFAD transgenic mice overexpressing ITPKB in neurons. (**A**) *Top*: immunodetection of ITPKB protein with an ITPKB antibody on brain sections from 6-month-old 5XFAD and 2Tg 5XFAD mice. *Bottom*: higher-magnification images of hippocampus (*left*) and cortex (*right*) neurons in 2Tg 5XFAD mice. Scale bars = 500 μm (*top*) and 50 μm (*bottom*). (**B**) *Top*: immunodetection of transgenic APP with an APP antibody on brain sections from 6-month-old 5XFAD and 2Tg 5XFAD mice. *Bottom*: higher magnification images of hippocampus (*left*) and cortex (*right*) in 5XFAD and 2Tg 5XFAD mice. Scale bars = 500 μm (*top*) and 50 μm (*bottom*). (**C**) Immunodetection of astrocytes with a GFAP antibody on brain sections from 6-month-old 5XFAD and 2Tg 5XFAD mice. Scale bars = 500 μm. Graph on the right represent the labelling index of GFAP in 6-month-old 5XFAD and 2Tg 5XFAD mice. The labelling index is defined as the GFAP-positive area related to the investigated cortex area. Means ± SEM are shown, 9–10 mice per group. *$P < 0.05$ by Student's *t*-test.

Downloaded from https://academic.oup.com/brain/article/137/2/537/283818 by guest on 23 April 2024

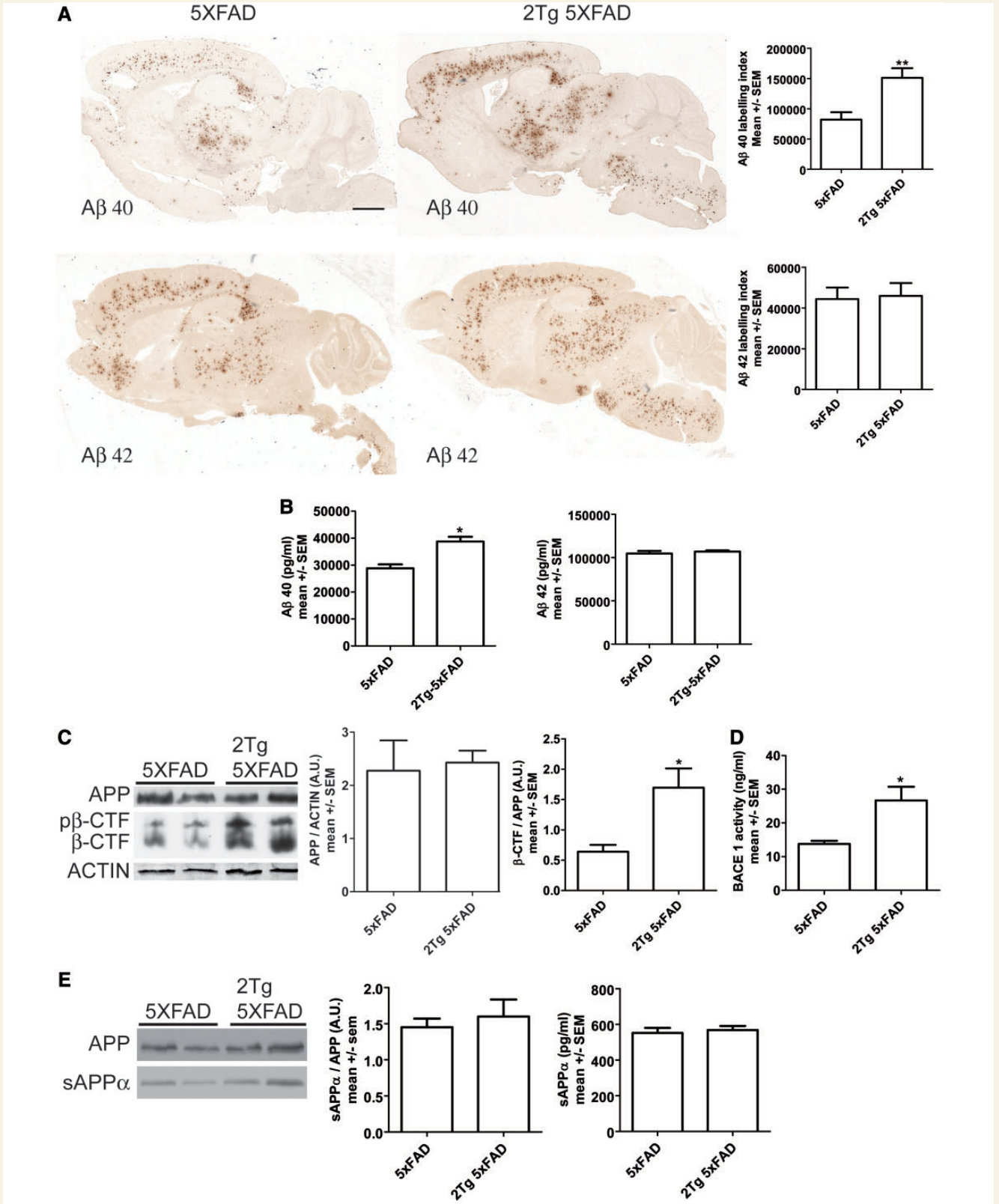

Figure 5 Increased amyloid-β_{40} (Aβ) peptide amyloid plaques density in 5XFAD transgenic mice overexpressing ITPKB in neurons. (**A**) Immunodetection of amyloid plaques with antibodies directed against amyloid-β_{40} or amyloid-β_{42} peptides in brain from 6-month-old 5XFAD (*left*) and 2Tg 5XFAD (*right*) mice. Graphs on the right represent the labelling index of amyloid-β_{40} and amyloid-β_{42} in 6-month-old 5XFAD and 2tg 5XFAD mice. The labelling index is defined as amyloid-β_{40}- and amyloid-β_{42}-positive areas related to the investigated cortex area. Means ± SEM are shown, 8–10 mice per group. $^{**}P < 0.01$ by Student's *t*-test. Scale bars = 500 μm. (**B**) Amyloid-β_{40} and amyloid-β_{42} peptides quantification by ELISA in insoluble formic acid fraction of brain homogenates from 6-month-old 5XFAD and 2Tg

(continued)

Downloaded from https://academic.oup.com/brain/article/137/2/537/283818 by guest on 23 April 2024

mechanistically, the altered ITPKB/Ins(1,3,4,5)P4/ERK signalling pathway detected in 2Tg 5XFAD mice is responsible for the increased BACE1 activity, amyloid-β peptides overproduction and tau hyperphosphorylation.

Decreased ERK activation is one of the mechanisms reported to explain the consequences of the absence of ITPKB and ITPKB-produced Ins(1,3,4,5)P4 on lymphoid cells development in ITPKB knock-out mice (Wen *et al*., 2004; Maréchal *et al*., 2007; Schurmans *et al*., 2011). Here, increased ITPKB expression in forebrain neurons of 5XFAD mice is associated with a significant increase in ERK activation. ERK activation is suspected to play an important role in Alzheimer's disease: active ERK is increased in Alzheimer's disease and represents one of the earliest events in disease pathogenesis (Arendt *et al*., 1995; Perry *et al*., 1999; Ferrer *et al*., 2001), ERK phosphorylates tau in cultured neuronal cells, in a brain slice model and in transgenic mice with an activated RAS/ERK pathway (Drewes *et al*., 1992; Lu *et al*., 1993; Garver *et al*., 1995; Holzer *et al*., 2001). Inhibition of ERK decreases tau phosphorylation and levels of soluble aggregated tau in tau transgenic mice (Le Corre *et al*., 2006). Furthermore, $Ser^{396/404}$ and Ser^{202}, but not Ser^{262}, are known ERK targets on tau protein (Biernat *et al*., 1993), and this kinase activity exactly matches the observed pattern of increased tau phosphorylation here in 2Tg 5XFAD brain homogenates. This increased tau phosphorylation is reminiscent of early stage Alzheimer's disease, in which phospho-tau proteins accumulate in neurons before aggregating in the form of paired helical filaments and neurofibrillary tangles. ERK also acts to phosphorylate target(s) that directly or indirectly increase BACE1 activity and expression, and thus modify APP metabolism in favour of increased production of amyloid-β peptides (Zuchner *et al*., 2004; Cho *et al*., 2007; Park *et al*., 2012). In 2Tg 5XFAD cortex homogenates, we observed that increased BACE1 activity and production of amyloid-β peptides are associated with an increased ERK activation; furthermore, treatment of *Itpkb*-transfected Neuro-2a cells with a MEK1/2 inhibitor completely prevented overproduction of amyloid-β peptides. Taken together, our results indicate that ERK overactivation plays an important role in the phenotype of 2Tg 5XFAD mice and of *Itpkb*-transfected Neuro-2a cells, and that a similar pathway involving ITPKB, ITPKB-produced Ins(1,3,4,5)P4 and ERK probably controls lymphocyte development and modulates Alzheimer pathology in mice.

Interestingly, 2Tg 5XFAD mice presented a striking amyloid-β peptide pattern characterized by a unique amyloid-β_{40} peptide overproduction. This peptide pattern probably results from an increased production specifically at the trans-Golgi network, where the amyloid-β_{40} peptide seemed to be produced (Hartmann *et al*., 1997; Choy *et al*., 2012). It is noteworthy that in *Itpkb*-tranfected Neuro-2a APP cells, ITPKB subcellular localization seems to play an important role since ITPKB amino-terminal end truncation affected both subcellular localization and amyloid-β_{40} peptide overproduction. Subcellular localization may also explain the absence of amyloid-β peptide overproduction in *Itpka*-transfected Neuro-2a cells, as ITPKA and ITPKB showed specific intracellular localization when expressed in Cos-7 cells (Dewaste *et al*., 2003). Even if the amyloid-β_{40} peptide is classically considered as less toxic than the amyloid-β_{42} peptide, increased amyloid-β_{40} plaque formation in 2Tg 5XFAD mice is not benign and may influence local neuritic dystrophy and gliosis, and eventually lead to disturbed neural network activity (Mayford *et al*., 1996; Tsai *et al*., 2004).

Interestingly, 5XFAD mice and a minority of patients with Alzheimer's disease tested in our study do not exhibit a marked increase in ITPKB protein expression in the cerebral cortex, as compared with control mice and subjects, suggesting that increased ITPKB expression is not a downstream effect of amyloid-β overproduction. The absence of increased ITPKB levels in 5XFAD mice might be explained by the fact that 5XFAD mice are a model of amyloid-β amyloidosis, engineered by overexpression of mutants APP and PSEN1, but not a full model for the physiopathology of sporadic Alzheimer's disease; this suggests that increased ITPKB expression is not an obligatory downstream effect of amyloid-β overproduction. The reason which determines the presence or the absence of ITPKB protein overexpression in Alzheimer cerebral cortex is currently unknown, but warrants genetic studies. On the other hand, identification of patients with Alzheimer's disease expressing a high level of ITPKB protein could lead to new treatment using ITPKB catalytic inhibitors to reduce production of amyloid-β peptides, plaque density and tau phosphorylation, three hallmarks of Alzheimer's disease. Such catalytic inhibitors have recently been discovered and shown to be active *in vitro* in cell culture and *in vivo* in mice (Miller *et al*., 2011).

Figure 5 Continued

5XFAD mice. Results are means ± SEM of four to five mice and represent the fold increased amyloid-β_{40} and amyloid-β_{42} peptides concentrations relative to 5XFAD mice. No amyloid-β_{40} or amyloid-β_{42} peptide was found in C57BL/6 control and in 2Tg mice (data not shown). *$P < 0.05$ by Mann Whitney test. (**C**) Immunodetection of APP β-CTF with the 6E10 carboxy-terminal end-specific APP antibody in brain homogenates from 6-month-old 2Tg 5XFAD ($n = 5$) and 5XFAD ($n = 4$) mice (*left*). Actin served as loading control. The graph on the *left* represents the quantification of APP signal relative to ACTIN signal and the graph on the *right* represents the quantification of the β-CTF signal relative to the APP signal. Means ± SEM are represented. *$P < 0.05$ by Mann Whitney test. (**D**) BACE1 activity was analysed by ELISA in brain homogenates from 5XFAD ($n = 4$) and 2Tg 5XFAD ($n = 3$) mice. Results represent the concentration of BACE1. *$P < 0.05$ by Student's *t*-test. (**E**) Immunodetection of soluble APPα and APP full-length protein with the 6E10 carboxy-terminal end-specific APP antibody in brain homogenates from 6-month-old 2Tg 5XFAD and 5XFAD mice (*left*). Graph in the *middle* represents the quantification of soluble APPα signal relative to the APP signal. Results are means ± SEM of three to four mice. Graph on the *right* panel: soluble APPα concentrations were determined by ELISA in soluble protein fraction of brain homogenates. Results are expressed as mean ± SEM of pg/ml of soluble APPα.

Downloaded from https://academic.oup.com/brain/article/137/2/537/283818 by guest on 23 April 2024

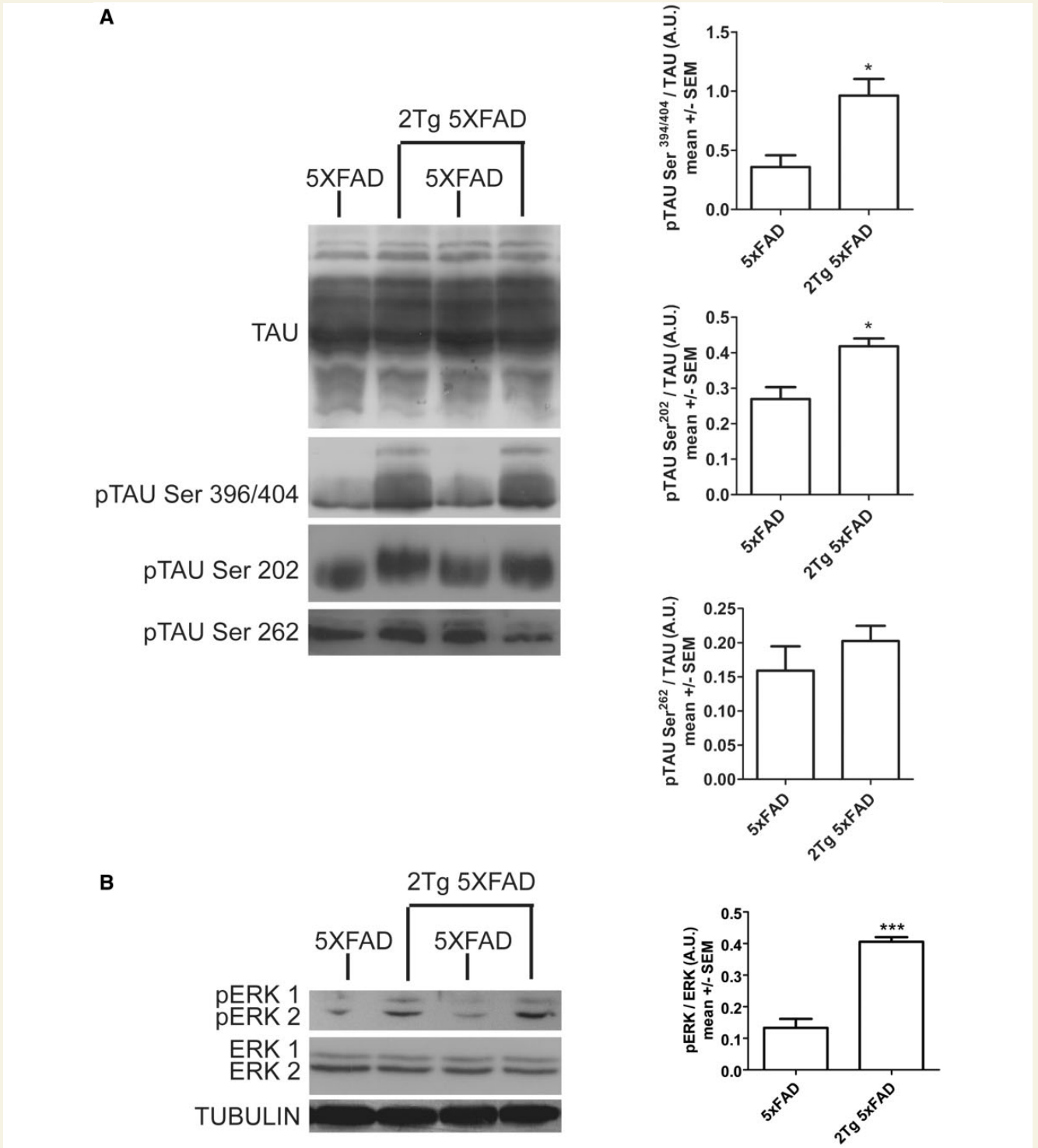

Figure 6 Increased tau and ERK1/2 phosphorylation in 5XFAD transgenic mice overexpressing ITPKB in neurons. (**A**) Immunodetection of tau proteins in brain homogenates from 6-month-old 2Tg 5XFAD ($n = 5$) and 5XFAD mice ($n = 4$). Antibodies directed against tau, phospho-tau (pTAU) Ser396/404, phospho-tau Ser202 and phospho-tau Ser262 proteins were used. Total tau protein served as loading control. Graphs represent the quantification of the phospho-tau signals relative to the tau signal. Means ± SEM are represented. $^*P < 0.05$ by Student's *t*-test. (**B**) Immunodetection of ERK1/2 proteins in brain homogenates from 6-month-old 2Tg 5XFAD ($n = 5$) and 5XFAD mice ($n = 4$). Antibodies directed against ERK1/2 and phosphoERK1/2 (pERK1/2) were used. Tubulin served as loading control. The graph represents the quantification of the phosphorylated (p)ERK1/2 signals relative to the total ERK1/2 signal. Means ± SEM are represented. $^{***}P < 0.001$ by Student's *t*-test.

Downloaded from https://academic.oup.com/brain/article/137/2/537/283818 by guest on 23 April 2024

In conclusion, our *in vitro* and *in vivo* results indicate that ITPKB and Ins(1,3,4,5)P4, its reaction product, control cell death, production of amyloid-β peptides, plaque density and tau hyperphosphorylation when overexpressed, as in a majority of patients with Alzheimer's disease, in neurons. They indicate that the involved mechanisms rely on an increase in ERK activation, leading to an increased BACE1 activity and tau hyperphosphorylation, and thus pointing to probable common signalling pathways downstream of ITPKB and Ins(1,3,4,5)P4 in neurons and lymphocytes. Finally, they suggest that ITPKB catalytic inhibitors could be of potential interest for reducing pathology in specific human patients with Alzheimer's disease with increased cortical ITPKB expression.

Acknowledgements

We thank G. Thinakaran for Neuro-2a-APP cells, R. Vassar for the 5XFAD mice, the team of the animal facility for mice husbandry.

Funding

This work was supported by the Fonds de la Recherche Scientifique-FNRS (FRS-FNRS to V.P. and S. S.), the Fonds pour la Formation à la Recherche dans l'Industrie et l'Agriculture (FRIA, to V.S.), the Fonds de la Recherche Scientifique Médicale (FRSM, to S. S., C. E. and J.P.B.), Action de Recherche Concertée de la Communauté française de Belgique (ARC; to S.S.), The Université Libre de Bruxelles (ULB, to V.S.), the Interuniversity Attraction Poles program of the Belgian Federal Science Policy Office (BELSPO) (IAP, to J.P.B), and the Diane program (Walloon region, to J.P.B). Some of the human brain tissue samples were provided by the GIE NeuroCEB Brain Bank (France Alzheimer, France Parkinson, ARSEP, CSC).

Supplementary material

Supplementary material is available at *Brain* online.

References

Arendt T, Holzer M, Grossmann A, Zedlick D, Bruckner MK. Increased expression and subcellular translocation of the mitogen activated protein kinase kinase and mitogen-activated protein kinase in Alzheimer's disease. Neuroscience 1995; 68: 5–18.

Biernat J, Gustke N, Drewes G, Mandelkow EM, Mandelkow E. Phosphorylation of Ser262 strongly reduces binding of TAU to microtubules: distinction between PHF-like immunoreactivity and microtubule binding. Neuron 1993; 11: 153–63.

Braak H, Braak E. Neuropathological stageing of Alzheimer-related changes. Acta Neuropathol (Berl.) 1991; 82: 239–59.

Brion JP, Guilleminot J, Couchie D, Flament-Durand J, Nunez J. Both adult and juvenile TAU microtubule-associated proteins are axon specific in the developing and adult rat cerebellum. Neuroscience 1988; 25: 139–46.

Cho HJ, Kim SK, Jin SM, Hwang EM, Kim YS, Huh K, et al. I. IFN-γ-induced BACE1 expression is mediated by activation of JAK2 and ERK1/2 signaling pathways and direct binding of STAT1 to BACE1 promoter in astrocytes. Glia 2007; 55: 253–62.

Choy RW-Y, Cheng Z, Schekman R. Amyloid precursor protein (APP) traffics from the cell surface via endosomes for amyloid β (Aβ) production in the *trans*-Golgi network. Proc Natl Acad Sci USA 2012; 109: E2077–82.

Communi D, Vanweyenberg V, Erneux C. Molecular study and regulation of D-myo-inositol 1,4,5-trisphospahte 3-kinase. Cell Signal 1995; 7: 643–50.

Dewaste V, Moreau C, De Smedt F, Bex F, De Smedt H, Wuytack F, et al. The three isoenzymes of human inositol-1,4,5-trisphosphate 3-kinase show specific intracellular localization but comparable Ca^{2+} responses on transfection in Cos-7 cells. Biochem J 2003; 374: 41–9.

Drewes G, Lichtenberg-Kraag B, Döring F, Mandelkow EM, Biernat J, Goris J, et al. Mitogen activated protein (MAP) kinase transforms TAU protein into an Alzheimer-like state. EMBO J 1992; 11: 2131–8.

Emilsson L, Saetre P, Jazin E. Alzheimer's disease: mRNA expression profiles of multiple patients show alterations of genes involved with calcium signaling. Neurobiol Dis 2006; 21: 618–25.

Ferrer I, Blanco R, Carmona M, Ribera R, Goutan E, Puig B, et al. Phosphorylated map kinase (ERK1, ERK2) expression is associated with early TAU deposition in neurones and glial cells, but not with increased nuclear DNA vulnerability and cell death, in Alzheimer's disease, Pick's disease, progressive supranuclear palsy and corticobasal degeneration. Brain Pathol 2001; 11: 144–58.

Garver TD, Oyler GA, Harris KA, Polavarapu R, Damuni Z, Lehman RA, et al. TAU phosphorylation in brain slices: pharmacological evidence for convergent effects of protein phosphatases on TAU and mitogen-activated protein kinase. Mol Pharmacol 1995; 47: 745–56.

Harold D, Abraham R, Hollingworth P, Sims R, Gerrish A, Hamshere ML, et al. Genome-wide association study identifies variants at CLU and PICALM associated with Alzheimer's disease. Nat Genet 2009; 4: 1088–93.

Hartmann T, Bieger SC, Brühl B, Tienari PJ, Ida N, Allsop D, et al. Distinct sites of intracellular production for Alzheimer's disease Aβ40/42 amyloid peptides. Nat Med 1997; 9: 1016–20.

Hascakova-Bartova R, Pouillon V, Dewaste V, Moreau C, Jacques C, Banting G, et al. Identification and subcellular distribution of endogenous Ins(1,4,5)P3 3-kinase B in mouse tissues. Biochem Biophys Res Commun 2004; 323: 920–5.

Holzer M, Rödel L, Seeger G, Gärtner U, Narz F, Janke C, et al. Activation of mitogen-activated protein kinase cascade and phosphorylation of cytoskeletal proteins after neurone-specific activation of p21ras. II. Cytoskeletal proteinsand dendritic morphology. Neuroscience 2001; 105: 1041–54.

Huang Y, Lennart M. Alzheimer mechanisms and therapeutic strategies. Cell 2012; 148: 1205–22.

Irvine RF, Schell MJ. Back in the water: the return of the inositol phosphates. Nat Rev Mol Cell Biol 2001; 2: 327–38.

Jia Y, Subramanian KK, Erneux C, Pouillon V, Hattori H, Jo H, You J, et al. Ins(1,3,4,5)P4 negatively regulates PtdIns(3,4,5)P3 signaling in neutrophils. Immunity 2007; 27: 453–67.

Jia Y, Loison F, Hattori H, Li Y, Erneux C, Park SY, et al. Inositol trisphosphate 3-kinase B (InsP3KB) as a physiological modulator of myelopoiesis. Proc Natl Acad Sci USA 2008; 105: 4739–44.

Lambert JC, Heath S, Even G, Campion D, Sleegers K, Hiltunen M, et al. Genome-wide association study identifies variants at CLU and CR1 associated with Alzheimer's disease. Nat Genet 2009; 4: 1094–9.

Le Corre S, Klafki HW, Plesnila N, Hübinger G, Obermeier A, Sahagún H, et al. An inhibitor of TAU hyperphosphorylation prevents severe motor impairments in TAU transgenic mice. Proc Natl Acad Sci USA 2006; 103: 9673–8.

Leroy K, Ando K, Laporte V, Dedecker R, Suain V, Authelet M, et al. Lack of TAU proteins rescues neuronal cell death and decreases amyloidogenic processing of APP in APP/PS1 mice. Am J Pathol 2012; 181: 1928–40.

Lu Q, Wood JG. Functional studies of Alzheimer's disease TAU protein. J Neurosci 1993; 13: 508–15.

Macq AF, Czech C, Essalmani R, Brion JP, Maron A, Mercken L, et al. The long term adenoviral expression of the human amyloid precursor

Downloaded from https://academic.oup.com/brain/article/137/2/537/283818 by guest on 23 April 2024

protein shows different secretase activities in rat cortical neurons and astrocytes. J Biol Chem 1998; 273: 28931–6.

Maréchal Y, Pesesse X, Jia Y, Pouillon V, Pérez-Morga D, Daniel J, et al. Inositol 1,3,4,5-tetrakisphosphate controls proapoptotic Bim gene expression and survival in B cells. Proc Natl Acad Sci USA 2007; 104: 13978–83.

Maréchal Y, Quéant S, Polizzi S, Pouillon V, Schurmans S. Inositol 1,4,5-trisphosphate 3-kinase B controls survival and prevents anergy in B cells. Immunobiol 2011; 216: 103–109.

Mayford M, Bach ME, Huang YY, Wang L, Hawkins RD, Kandel ER. Control of memory formation through regulated expression of a CaMKII transgene. Science 1996; 274: 1678–83.

Miller AT, Sandberg M, Huang YH, Young M, Sutton S, Sauer K, et al. Production of Ins(1,3,4,5)P4 mediated by the kinase Itpkb inhibits store-operated calcium channels and regulates B cell selection and activation. Nat Immunol 2007; 8: 514–21.

Miller AT, Sandberg M, Wen B, Pan S, Beisner DR, Tian S-S, et al. Novel LMW inhibitors of ITPKB confirm an essential role for IP4 in controlling lymphocyte development and activation. In: Conference on Inositide Signaling in Pharmacology and Disease Keystone Symposium, Keystone, CO, USA, 2011.

Mirra SS, Heyman A, McKeel D, Sumi SM, Crain BJ, Brownlee LM, et al. The Consortium to Establish a Registry for Alzheimer's Disease (CERAD). Part II. Standardization of the neuropathologic assessment of Alzheimer's disease. Neurology 1991; 41: 479–86.

Morel M, Authelet M, Dedecker R, Brion JP. Glycogen synthase kinase-3beta and the p25 activator of cyclin dependent kinase 5 increase pausing of mitochondria in neurons. Neuroscience 2010; 167: 1044–56.

Oakley H, Cole SL, Logan S, Maus E, Shao P, Craft J, et al. Intraneuronal β-amyloid aggregates, neurodegeneration, and neuron loss in transgenic mice with five familial Alzheimer's disease mutations: potential factors in amyloid plaque formation. J Neurosci 2006; 26: 10129–40.

Park MH, Choi DY, Jin HW, Yoo HS, Han JY, Oh KW, et al. Mutant presenilin 2 increases β-secretase activity through reactive oxygen species-dependent activation of extracellular signal-regulated kinase. J Neuropathol Exp Neurol 2012; 71: 130–9.

Pattni K, Banting G. Ins(1,4,5)P3 metabolism and the family of IP3-3 kinases. Cell Signal 2004; 16: 643–54.

Perry G, Roder H, Nunomura A, Takeda A, Friedlich AL, Zhu X, et al. Activation of neuronal extracellular receptor kinase (ERK) in Alzheimer's disease links oxidative stress to abnormal phosphorylation. Neuroreport 1999; 10: 2411–15.

Pouillon V, Hascakova-Bartova R, Pajak B, Adam E, Bex F, Dewaste V, et al. Inositol 1,3,4,5-tetrakisphosphate is essential for T lymphocyte development. Nat Immunol 2003; 4: 1136–143.

Schurmans S, Pouillon V, Maréchal Y. Regulation of B cell survival, development and function by inositol 1,4,5-trisphosphate 3-kinase B (Itpkb). Adv Enz Reg 2011; 51: 66–73.

Sauer K, Park E, Siegemund S, French AR, Wahle JA, Sternberg L, et al. Inositol tetrakisphosphate limits NK cell effector functions by controlling phosphoinositide 3-kinase signaling. Blood 2013; 121: 286–97.

Takazawa K, Lemos M, Delvaux A, Lejeune C, Dumont JE, Erneux C. Rat brain inositol 1,4,5-trisphosphate 3-kinase. $Ca^{2(+)}$-sensitivity, purification and antibody production. Biochem J 1990; 268: 213–17.

Thinakaran G, Teplow DB, Siman R, Greenberg B, Sisodia SS. Metabolism of the "Swedish" amyloid precursor protein variant in Neuro2a (N2a) cells. J Biol Chem 1996; 271: 9390–7.

Tsai J, Grutzendler J, Duff K, Gan WB. Fibrillar amyloid deposition leads to local synaptic abnormalities and breakage of neuronal branches. Nat Neurosci 2004; 7: 1181–3.

Vanweyenberg V, Communi D, D'Santos CS, Erneux C. Tissue- and cell-specific expression of Ins(1,4,5)P3 3-kinase isoenzymes. Biochem J 1995; 306: 429–35.

Wen BG, Pletcher MT, Warashina M, Choe SH, Ziaee N, Wiltshire T, et al. Inositol (1,4,5) trisphosphate 3 kinase B controls positive selection of T cells and modulates ERK activity. Proc Natl Acad Sci USA 2004; 101: 5604–9.

York JD, Guo S, Odom AR, Spiegelberg BD, Stolz LE. An expended view of inositol signaling. Adv Enzyme Regul 2001; 41: 57–71.

Zuchner T, Perez-Polo JR, Schliebs R. β-secretase BACE1 is differentially controlled through muscarinic acetylcholine receptor signling. J Neurosci Res 2004; 77: 250–257.

Downloaded from https://academic.oup.com/brain/article/137/2/537/283818 by guest on 23 April 2024